Electronic Transactions on Numerical Analysis.
Volume 32, pp. 90-105, 2008.

ISSN 1068-9613.

ETNA
Kent State University
etna@mcs.kent.edu

STABILIZATION OF LOCAL PROJECTION TYPE APPLIED TO CONVECTION-DIFFUSION PROBLEMS WITH MIXED BOUNDARY CONDITIONS*

GUNAR MATTHIES†, PIOTR SKRZYPACZ‡, AND LUTZ TOBISKA‡

Abstract. We present the analysis for the local projection stabilization applied to convection-diffusion problems with mixed boundary conditions. We concentrate on the enrichment approach of the local projection methods. Optimal a-priori error estimates will be proved. Numerical tests confirm the theoretical convergence results. Moreover, the local projection stabilization leads to numerical schemes which work well for problems with several types of layers. Away from layers, the solution is captured very well.

Key words. stabilized finite elements, convection-diffusion

AMS subject classifications. 65N12, 65N30

1. Introduction. Convection-diffusion equations occur for instance if physical processes in chemical engineering are modelled. Depending on the problem, different types of boundary conditions are applied on different parts of the domain boundary. A common feature of these problems is the small diffusion coefficient, i.e., the process is convection and/or reaction dominant. Since standard Galerkin discretisations will produce unphysical oscillations for this type of problems, stabilization techniques have been developed. The streamline-upwind Petrov–Galerkin method (SUPG) has been successfully applied to convection-diffusion problems. It was proposed by Hughes and Brooks [19]. One fundamental drawback of SUPG is that several terms which include second order derivatives have to be added to the standard Galerkin discretisation in order to ensure consistency. Alternatively, continuous interior penalty methods [1, 6], residual free bubble methods [10, 11, 12], or subgrid modelling [8, 18] can be used for stabilizing the discretised convection-diffusion problems.

We will focus in this paper on the local projection stabilization. This method has been proposed for the Stokes problem in [3]. The extension to the transport problem was given in [4]. The analysis of the local projection method applied to equal-order interpolation discretisation of the Oseen problem can be found in [5, 23]. We will apply the local projection method to convection-diffusion problems. The stabilization term of the local projection method is based on a projection $\pi_h : V_h \to D_h$ of the finite element space V_h which approximates the solution into a discontinuous space D_h. The standard Galerkin discretisation is stabilized by adding a term which gives L^2 control over the fluctuation $id - \pi_h$ of the gradient of the solution.

Originally, the local projection technique was proposed as a two-level method where the projection space D_h is defined on a coarser grid. The drawback of this approach is an increased discretisation stencil. The general approach given in [13, 23] allows to construct local projection methods, such that the discretisation stencil is not increased compared to the standard Galerkin or the SUPG approach since the approximation space Y_h and the projection space D_h are defined on the same mesh. In this case, the approximation space Y_h is

*Received November 27, 2007. Accepted for publication May 2, 2008. Published online on February 2, 2009. Recommended by A. Rösch. This work was partially supported by the German Research Foundation (DFG) through grants To143 and FOR 447.

†Fakultät für Mathematik, Ruhr-Universität Bochum, Universitätsstraße 150, D-44780 Bochum, Germany (`Gunar.Matthies@ruhr-uni-bochum.de`).

‡Institut für Analysis und Numerik, Otto-von-Guericke-Universität Magdeburg, Postfach 4120, D-39016 Magdeburg, Germany (`piotr.skrzypacz, tobiska@mathematik.uni-magdeburg.de`).

ETNA
Kent State University
etna@mcs.kent.edu

enriched compared to standard finite element spaces. We will concentrate in this paper on the enrichment approach of the local projection method.

The main objective of this paper is to provide a convergence theory for the local projection method applied to convection-diffusion problems with mixed boundary conditions. For sufficiently regular solutions the same a-priori error estimates which are known for SUPG are proven. Furthermore, several test problems with different types of interior and boundary layers will be presented. They show that the local projection stabilization allows to obtain numerical solutions which capture the solution away from layers.

The plan of this paper is as follows. Section 2 introduces the considered problem class, the weak formulation, and the local projection stabilization. An a-priori error estimate for the stabilized discrete problem will be given in Section 3. Numerical results for problems with different type of layers will be presented in Section 4. Conclusions will be given in Section 5.

We use the following notation in this paper. The convection-diffusion problem is considered in a bounded domain $\Omega \subset \mathbb{R}^d$, $d = 2, 3$, with polygonal or polyhedral boundary $\partial\Omega$. For a set D which is either a d-dimensional measurable subset of Ω or a $(d-1)$-dimensional measurable subset of $\partial\Omega$, the fractional order spaces $H^s(D)$, $s \in [0,\infty)$ with norm $\|\cdot\|_{s,D}$ and seminorm $|\cdot|_{s,D}$ will be used. For $s = m \in \mathbb{N}_0$, the space $H^s(D)$ is defined as the Sobolev space $H^s(D) := W^{m,2}(D)$ with norm $\|\cdot\|_{s,D} = \|\cdot\|_{m,2,D}$ and seminorm $|\cdot|_{s,D} = |\cdot|_{m,2,D}$. For non-integer $s = m + \lambda$ with $m \in \mathbb{N}_0$ and $\lambda \in (0,1)$, the space $H^s(D)$ is defined as the Sobolev-Slobodeckij space $H^s(D) := W^{m+\lambda,2}(D)$, which consists of all functions from the Sobolev space $W^{m,2}(D)$, such that

$$|v|_{m+\lambda,2,D} := \left(\sum_{|\alpha|=m} \int_D \int_D \frac{|D^\alpha v(x) - D^\alpha v(y)|^2}{\|x-y\|^{d+2\lambda}} \, dx dy \right)^{1/2} < \infty .$$

The Sobolev-Slobodeckij space $W^{m+\lambda,2}(D)$ is equipped with the norm

$$\|v\|_{m+\lambda,2,D} := \left(\|v\|^2_{m,2,D} + |v|^2_{m+\lambda,2,D} \right)^{1/2} .$$

As usual, we set $\|\cdot\|_{s,D} = \|\cdot\|_{m+\lambda,2,D}$ and $|\cdot|_{s,D} = |\cdot|_{m+\lambda,2,D}$. The L^2 inner product over $G \subset \Omega$ and $\Gamma \subset \partial\Omega$ will be denoted by $(\cdot,\cdot)_G$ and $\langle \cdot,\cdot \rangle_\Gamma$, respectively. In case $G = \Omega$ the index G will be omitted. For $k \geq 0$ and a d-dimensional subset $G \subset \Omega$, let $P_k(G)$ denote the space of polynomials of degree less than or equal to k while $Q_k(G)$ is the space of all polynomials of degree less than or equal to k in each variable separately.

Throughout this paper, C will denote a generic constant which is independent of the mesh and the diffusion parameter ε. We will use the notation $\alpha \sim \beta$ if there are positive constants C_1 and C_2, such that $C_1\beta \leq \alpha \leq C_2\beta$ holds.

2. Model problem and local projection method.

2.1. Weak formulation. We consider the scalar convection-diffusion problem with mixed boundary conditions

$$\left\{ \begin{aligned} -\varepsilon\Delta u + \boldsymbol{b}\cdot\nabla u + cu &= f && \text{in } \Omega, \\ u &= g_D && \text{on } \Gamma_D, \\ \varepsilon\frac{\partial u}{\partial \boldsymbol{n}} &= g_N && \text{on } \Gamma_N, \end{aligned} \right. \tag{2.1}$$

where $\varepsilon > 0$ is a small constant. The boundary $\partial\Omega$ of Ω consists of two disjoint parts, the Dirichlet part Γ_D and the Neumann part Γ_N. Let Γ_N be a relatively open C^1 part of $\partial\Omega$

and $\Gamma_D = \partial\Omega \setminus \Gamma_N$. The unit outer normal vector with respect to $\partial\Omega$ is denoted by $\boldsymbol{n}$. We are looking for the distribution of concentration u in Ω. The reaction coefficient $c \in L^\infty(\Omega)$ is assumed to be non-negative. Let $f \in L^2(\Omega)$, $g_D \in H^{1/2}(\Gamma_D)$, $g_N \in H^{-1/2}(\Gamma_N)$ be given functions. Furthermore, we require that the convection field $\boldsymbol{b} \in \left(W^{1,\infty}(\Omega)\right)^d$ and the reaction coefficient c fulfil for some $c_0 > 0$ the following condition

$$c(x) - \frac{1}{2}\nabla \cdot \boldsymbol{b}(x) \geq c_0 > 0 \qquad \forall x \in \overline{\Omega}. \tag{2.2}$$

We assume also that the inflow boundary is part of the Dirichlet boundary, i.e.,

$$\big\{x \in \partial\Omega \,:\, (\boldsymbol{b}\cdot\boldsymbol{n})(x) < 0\big\} \subset \Gamma_D. \tag{2.3}$$

We define the function spaces

$$V = H^1(\Omega) \quad \text{and} \quad V_0 = \{v \in V :\, v|_{\Gamma_D} = 0\}.$$

A weak formulation of (2.1) reads:

Find $u \in V$ with $u|_{\Gamma_D} = g_D$, such that

$$a(u,v) = (f,v) + \langle g_N, v\rangle_{\Gamma_N} \quad \forall\, v \in V_0, \tag{2.4}$$

where the bilinear form $a : H^1(\Omega) \times H^1(\Omega) \to \mathbb{R}$ is defined by

$$a(u,v) = \varepsilon\,(\nabla u, \nabla v) + (\boldsymbol{b}\cdot\nabla u, v) + (cu, v). \tag{2.5}$$

The conditions (2.2) and (2.3) guarantee the V_0-coercivity of the bilinear form a. The existence and uniqueness of a weak solution of problem (2.4) can be concluded from the Lax–Milgram lemma. For details, we refer to [15].

It is well-known that for pure Dirichlet boundary data, the weak solution of a two-dimensional problem belongs to $H^2(\Omega)$ provided that the domain is convex; see [16, 17]. However, in general, we can not expect that the weak solution of the problem (2.1) is in $H^2(\Omega)$. Indeed, in the two-dimensional case, the solution of the Poisson equation ($\varepsilon = 1$, $b = c = 0$) with homogenuous Dirichlet data behaves in the neighbourhoood of a vertex of the boundary with inner angle α like $u_1 := r^{\pi/\alpha}\Phi(\varphi)$ and with mixed Dirichlet-Neumann data like $u_2 := r^{\pi/(2\alpha)}\Phi(\varphi)$. Here, (r,φ) denotes a local system of polar coordinates where r is the distance to the boundary vertex, $\varphi \in [0,\alpha]$, and $\Phi(\cdot)$ is a smooth function. From [16, Theorem 1.4.5.3] we conclude that $u_1 \in H^s$ locally if and only if $s < \pi/\alpha + 1$ provided that $\pi/\alpha \notin \mathbb{N}$. Analogously, for $\pi/(2\alpha) \notin \mathbb{N}$ we get $u_2 \in H^s$ locally if and only if $s < \pi/(2\alpha) + 1$.

2.2. Local projection method. For the finite element discretisation of (2.4), we are given a shape regular family $\{\mathcal{T}_h\}$ of decomposition of Ω into d-simplices, quadrilaterals, or hexahedra. The diameter of K will be denoted by h_K and the mesh size parameter h is defined by $h := \max_{K\in\mathcal{T}_h} h_K$. For $\mathcal{T}_h$, let $\mathcal{E}_{h,N}$ denote the set of all edges/faces of cells $K \in \mathcal{T}_h$ which belong to Γ_N.

Let $V_h \subset V$ be a finite element space of continuous elements of order $r \geq 1$. We fix the polynomial order r and the dependence of constants on r will not be elaborated in this paper. Let

$$V_{0,h} = \{v \in V_h :\, v_h|_{\Gamma_D} = 0\}$$

be the discrete test space.

ETNA
Kent State University
etna@mcs.kent.edu

Since the standard Galerkin discretisation of (2.4) lacks generally stability in the convection dominated regime $\varepsilon \ll 1$, unphysical oscillations will appear in the discrete solution. To circumvent this problem, we consider the stabilization by the local projection method. Let $D_h(K)$, $K \in \mathcal{T}_h$, be finite dimensional spaces and $\pi_K : L^2(K) \to D_h(K)$ the local L^2 projections into $D_h(K)$. The projection space D_h is given by

$$D_h := \bigoplus_{K \in \mathcal{T}_h} D_h(K).$$

We define the global projection operator $\pi_h : L^2(\Omega) \to D_h$ by $(\pi_h w)|_K = \pi_K(w|_K)$. The fluctuation operator $\kappa_h : L^2(\Omega) \to L^2(\Omega)$ is given by

$$\kappa_h := id - \pi_h,$$

where $id : L^2(\Omega) \to L^2(\Omega)$ is the identity mapping in $L^2(\Omega)$. Note that all operators will be applied componentwise to vector-valued functions.

We define the stabilizing term

$$S_h(u_h, v_h) := \sum_{K \in \mathcal{T}_h} \tau_K \big(\kappa_h(\nabla u_h), \kappa_h(\nabla v_h)\big)_K, \tag{2.6}$$

where τ_K, $K \in \mathcal{T}_h$, denote user-defined parameters. Their choice will be discussed later on. Note that the stabilization term S_h gives control over the fluctuation of the gradient. An alternative way is to control by

$$\sum_{K \in \mathcal{T}_h} \tau_K \big(\kappa_h(\boldsymbol{b} \cdot \nabla u_h), \kappa_h(\boldsymbol{b} \cdot \nabla v_h)\big)_K,$$

which represents the fluctuation of the derivative in streamline direction. The proof of the convergence result in the next section shows that we need the assumption $c_0 > 0$ while using the stabilizing term (2.6). For the alternative choice, we can allow $c_0 = 0$ but additional regularity of $\boldsymbol{b}$ has to be assumed; see [23].

We can now state the local projection stabilization of the discretisation of (2.4) as follows:

Find $u_h \in V_h$ with $u_h|_{\Gamma_D} = g_{D,h}$, such that

$$a(u_h, v_h) + S_h(u_h, v_h) = (f, v_h) + \langle g_N, v_h \rangle_{\Gamma_N} \quad \forall\, v_h \in V_{0,h}, \tag{2.7}$$

where $g_{D,h}$ denotes a suitable approximation of g_D which will be discussed in the next section.

The local projection norm

$$|||v_h||| := \left\{ \varepsilon |v_h|_1^2 + c_0 \|v_h\|_0^2 + \frac{1}{2} \big\| |\boldsymbol{b} \cdot \boldsymbol{n}|^{1/2} v_h \big\|_{0,\Gamma_N}^2 + S_h(v_h, v_h) \right\}^{1/2} \tag{2.8}$$

will be used for our analysis.

The key point in the analysis of local projection methods is the existence of an interpolation operator j_h which provides the usual approximation properties and ensures that the interpolation error is orthogonal to D_h. In order to obtain error estimates in the most local form, we are interested in Lagrange interpolation which is defined on continuous functions only. We assume that the solution u of convection-diffusion problem with mixed boundary conditions (2.4) belongs to the Sobolev–Slobodeckij space $H^{1+\lambda}(\Omega)$ with $1 + \lambda > \frac{d}{2}$ which ensures the continuity of u. Let $j_h : H^{1+\lambda}(\Omega) \to V_h$ be an interpolation operator with

$$\|w - j_h w\|_{0,K} + h_K |w - j_h w|_{1,K} \le C h_K^{1+\lambda} \|w\|_{1+\lambda,K} \quad \forall w \in H^{1+\lambda}(\Omega), \tag{2.9}$$

and the following orthogonality relation

$$(w - j_h w, q_h) = 0 \quad \forall q_h \in D_h \ \forall w \in H^{1+\lambda}(\Omega). \tag{2.10}$$

We assume that $(j_h w)|_{\Gamma_D}$ depends only on $w|_{\Gamma_D}$. Let

$$Y_h(K) := \{w_h|_K \,:\, w_h \in V_h\} \cap H_0^1(K)$$

denote the local bubble part of the finite element space V_h on K.

A sufficient condition for existence of an interpolation operator fulfilling (2.9) and (2.10) provides the following lemma.

LEMMA 2.1 (Local inf-sup condition). *Let $i_h : H^{1+\lambda}(\Omega) \to V_h$, $1 + \lambda > \frac{d}{2}$, be an interpolation operator which provides for all $K \in \mathcal{T}_h$ the estimate*

$$\|w - i_h w\|_{0,K} + h_K |w - i_h w|_{1,K} \le C h_K^{1+\lambda} \|w\|_{1+\lambda,K} \quad \forall w \in H^{1+\lambda}(\Omega). \tag{2.11}$$

Furthermore, let the local inf-sup condition

$$\exists \beta_1 > 0 \ \forall h > 0 \ \forall K \in \mathcal{T}_h : \inf_{q_h \in D_h(K)} \sup_{v_h \in Y_h(K)} \frac{(v_h, q_h)_K}{\|v_h\|_{0,K} \|q_h\|_{0,K}} \ge \beta_1 > 0 \tag{2.12}$$

be satisfied. Then, there exists an interpolation operator $j_h : H^{1+\lambda}(\Omega) \to V_h$ possessing the approximation property (2.9) *and the orthogonality property* (2.10).

Proof. The construction of the interpolation operator j_h follows the way presented in the proof of Theorem 2.2 in [23]. □

The assumed estimate (2.11) holds true for the Lagrangian interpolator i_h on simplices; see [9]. Combining the ideas of [9] with results given in [24, 22] yields the above estimate on quadrilaterals and hexahedra. Moreover, we obtain

$$\|w - j_h w\|_{0,K} + h_K |w - j_h w|_{1,K} \le C h_K^{\min(s,r)+1} \|w\|_{\min(s,r)+1,K} \quad \text{for } w \in H^{s+1}(\Omega).$$

If $P_{r-1}(K) \subset D_h(K)$ holds true for some $r \ge 1$, then the property of the local L^2 projection π_K and interpolation theory in Sobolev–Slobodeckij spaces give the approximation property

$$\|\kappa_h q\|_{0,K} \le C h_K^{\min(s,r)} \|q\|_{\min(s,r),K} \qquad \forall q \in H^s(K). \tag{2.13}$$

In order to satisfy the local inf-sup condition (2.12), the local bubble space $Y_h(K)$ has to be sufficiently large compared to the local projection space $D_h(K)$. However, the minimal dimension of $D_h(K)$ is determined indirectly by (2.13).

Several families of pairs (V_h, D_h) of approximation spaces V_h and projection spaces D_h which provide the properties (2.9) and (2.10) were given in [23]. We recall here one family on quadrilaterals which was used for our calculations presented in Section 4. Let $F_K : \widehat{K} \to K$ be the multilinear mapping from the reference hyper-cube $\widehat{K} = (-1,1)^d$ onto the mesh cell $K \in \mathcal{T}_h$. The projection space D_h is chosen to be the mapped space

$$P_{r-1,h}^{\text{disc}} := \{v \in L^2(\Omega) \,:\, v|_K \circ F_K \in P_{r-1}(\widehat{K}) \ \forall K \in \mathcal{T}_h\}.$$

Let

$$\hat{b}(\hat{x}) = \prod_{i=1}^{d} (1 - \hat{x}_i^2), \qquad \hat{x} = (\hat{x}_1, \dots, \hat{x}_d) \in \widehat{K},$$

ETNA
Kent State University
etna@mcs.kent.edu

be the Q_2 bubble function defined on $\widehat{K}$. The usual local space $Q_r(\widehat{K})$ is enriched to

$$Q_r^{\text{bubble}}(\widehat{K}) := Q_r(\widehat{K}) \oplus \text{span}(\hat{b}\,\hat{x}_i^{r-1}\,,\ i = 1, \ldots, d).$$

The approximation space V_h is set to

$$Q_{r,h}^{\text{bubble}} := \{v \in H^1(\Omega)\ :\ v|_K \circ F_K \in Q_r^{\text{bubble}}(\widehat{K})\ \forall K \in \mathcal{T}_h\}.$$

For $r \geq 1$, the finite element pair $(V_h, D_h) = (Q_{r,h}^{\text{bubble}}, P_{r-1,h}^{\text{disc}})$ satisfies the inf-sup condition (2.12) of Lemma 2.1 and provides the interpolation error estimate from Lemma 2.1. Hence, there exists an interpolation operator j_h satisfying (2.9) and (2.10). For details, see Lemma 4.2 in [23].

Note that we have $P_{r-1}(K) \not\subset P_{r-1,h}^{\text{disc}}(K)$ for non-affine mappings $F_K : \widehat{K} \to K$ but the approximation property (2.13) holds for successively refined meshes, see [2, 21, 22].

3. Error analysis. Let us first discuss the choice of the discrete Dirichlet boundary condition $g_{D,h} \in \{v_h|_{\Gamma_D}\ :\ v_h \in V_h\}$. We use an interpolation of g_D which fits to the interpolation j_h, such that $g_{D,h} = (j_h u)|_{\Gamma_D}$ for the solution u of (2.4). This is possible since the restriction of the standard nodal interpolation onto Γ_D depends only on nodal values at Γ_D. For example, $g_{D,h}$ for the $Q_{r,h}^{\text{bubble}}$ discretisation is defined as the $Q_{r,h}$ interpolation of g_D on the boundary Γ_D.

We continue with solvability of the stabilized discrete problem (2.7).

LEMMA 3.1 (Solvability). *Let $g_{D,h} = (j_h u)|_{\Gamma_D}$. The stabilized discrete problem* (2.7) *possesses a unique solution.*

Proof. Since $g_D \in H^{1/2}(\Gamma_D)$ and $g_{D,h} \in \{v_h|_{\Gamma_D}\ :\ v_h \in V_h\}$, we can find some extension $\tilde{g}_{D,h}$, such that $\tilde{g}_{D,h} - u_h \in V_{0,h}$. Indeed, $\tilde{g}_{D,h} = j_h u$ is a possible choice. The key argument for showing the solvability of (2.7) is the proof of the coercivity of the stabilized bilinear form $a + S_h$ with respect to the local projection norm $|||\cdot|||$. Using the conditions (2.2) and (2.3), we obtain for all test functions $v_h \in V_{0,h}$

$$\begin{aligned}
(3.1)\quad a(v_h, v_h) &+ S_h(v_h, v_h) \\
&= \varepsilon\,|v_h|_1^2 + \frac{1}{2}\int_\Omega \boldsymbol{b}\cdot\nabla v_h^2\,dx + \int_\Omega c v_h^2\,dx + S_h(v_h, v_h) \\
&= \varepsilon|v_h|_1^2 + \frac{1}{2}\int_{\Gamma_N} (\boldsymbol{b}\cdot\boldsymbol{n})\,v_h^2\,ds + \int_\Omega \left(c - \frac{1}{2}\nabla\cdot\boldsymbol{b}\right)\,v_h^2\,dx + S_h(v_h, v_h) \\
&\geq |||v_h|||^2\,.
\end{aligned}$$

Hence, the existence and uniqueness of the discrete solution can be concluded from the Lax–Milgram lemma. ∎

We will investigate the consistency error which is caused by adding the stabilizing term S_h to the weak formulation.

LEMMA 3.2 (Consistency error). *Let u and u_h be solutions of the problems* (2.4) *and* (2.7)*, respectively. Then, the approximated Galerkin orthogonality*

$$(a + S_h)(u - u_h, w_h) = S_h(u, w_h) \quad \forall w_h \in V_{0,h} \tag{3.2}$$

holds true. Let $\tau_K \sim h_K$ and $u \in H^{1+\lambda}(\Omega)$. Then, the estimate

$$|S_h(u, v_h)| \leq C\left(\sum_{K\in\mathcal{T}_h} h_K^{2\lambda+1}\|u\|_{1+\lambda,K}^2\right)^{1/2} |||v_h||| \quad \forall v_h \in V_h \tag{3.3}$$

is satisfied. In the case $u \in H^{s+1}(\Omega)$*,* $s \geq 1$*, the estimate*

$$|S_h(u, v_h)| \leq C \left(\sum_{K \in \mathcal{T}_h} h_K^{2\min(s,r)+1} \|u\|^2_{\min(s,r)+1,K} \right)^{1/2} |||v_h||| \quad \forall v_h \in V_h \tag{3.4}$$

is obtained.

Proof. The relation (3.2) follows by subtracting (2.4) from (2.7). The Cauchy–Schwarz inequality implies

$$|S_h(u, v_h)| \leq S_h(u, u)^{1/2}\, S_h(v_h, v_h)^{1/2}$$

where the definition (2.6) of S_h was used. For $u \in H^{1+\lambda}(\Omega)$, it follows from (2.13) and $\tau_K \sim h_K$ that

$$S_h(u, u) = \sum_{K \in \mathcal{T}_h} \tau_K \|\kappa_h(\nabla u)\|^2_{0,K} \leq C \sum_{K \in \mathcal{T}_h} h_K^{2\lambda+1} \|u\|^2_{1+\lambda,K}.$$

Hence, we have

$$|S_h(u, v_h)| \leq C \left(\sum_{K \in \mathcal{T}_h} h_K^{2\lambda+1} \|u\|^2_{1+\lambda,K} \right)^{1/2} |||v_h|||$$

and the second assertion is proved. The last statement of this lemma follows analogously. □

Using the previous estimates, we are now able to formulate and prove our main convergence result.

THEOREM 3.3 (A-priori error estimate). *Assume* $\tau_K \sim h_K$*. Let* $u \in H^{1+\lambda}(\Omega)$ *and* $u_h \in V_h$ *be the solutions of problems* (2.4) *and* (2.7)*, respectively. Then, the a-priori error estimate*

$$|||u - u_h||| \leq C \left(\sum_{K \in \mathcal{T}_h} (\varepsilon + h_K) h_K^{2\lambda} \|u\|^2_{1+\lambda,K} \right)^{1/2} \tag{3.5}$$

holds true. If in addition $u \in H^{s+1}(\Omega)$*,* $s \geq 1$*, then the estimate*

$$|||u - u_h||| \leq C \left(\sum_{K \in \mathcal{T}_h} (\varepsilon + h_K) h_K^{2\min(s,r)} \|u\|^2_{\min(s,r)+1,K} \right)^{1/2} \tag{3.6}$$

is fulfilled.

Proof. First, the triangle inequality implies

$$|||u - u_h||| \leq |||u - j_h u||| + |||j_h u - u_h|||. \tag{3.7}$$

In order to proceed with the estimate of the interpolation error in the local projection norm, we provide some auxiliary results concerning the interpolation error on edges/faces and the fluctuation operator. We note the following trace estimate on any edge/face $E \subset \partial K$, $K \in \mathcal{T}_h$,

$$\|v\|_{0,E} \leq C h_K^{1/2} |v|_{1,K} + C h_K^{-1/2} \|v\|_{0,K} \quad \forall v \in H^1(K), \tag{3.8}$$

ETNA
Kent State University
etna@mcs.kent.edu

which gives immediately the local interpolation error estimate

$$\|j_h u - u\|_{0,E} \le C h_K^{\lambda+1/2} \|u\|_{1+\lambda,K} \tag{3.9}$$

on an edge/face $E \subset \partial K$. Furthermore, one can show for $\boldsymbol{b} \in \left(W^{1,\infty}(K)\right)^d$ the estimate

$$\begin{aligned} \|\kappa_h(\boldsymbol{b}\cdot\nabla v_h)\|_{0,K} &\le C|\boldsymbol{b}|_{1,\infty,K}\|v_h\|_{0,K} + \|\boldsymbol{b}\|_{0,\infty,K}\|\kappa_h(\nabla v_h)\|_{0,K} \\ &\le C\big(\|v_h\|_{0,K} + \|\kappa_h(\nabla v_h)\|_{0,K}\big); \end{aligned} \tag{3.10}$$

see the proof of Corollary 2.14 in [23].

Using the interpolation error estimates (2.9) and (3.9), the fact $\boldsymbol{b} \in \left(W^{1,\infty}(\Omega)\right)^d$, and the L^2 stability of the fluctuation operator κ_h, we conclude

$$|||u - j_h u||| \le C \left(\sum_{K\in\mathcal{T}_h} (\varepsilon + h_K^2 + \tau_K) h_K^{2\lambda} \|u\|_{1+\lambda,K}^2 \right)^{1/2}. \tag{3.11}$$

In order to estimate the second error term on the right hand side of (3.7), we use $u_h|_{\Gamma_D} = \big(j_h u\big)|_{\Gamma_D}$ and the $V_{0,h}$ coercivity proved in Lemma 3.1. We obtain by using relation (3.2) from Lemma 3.2

$$\begin{aligned} |||j_h u - u_h|||^2 &\le a(j_h u - u_h, w_h) + S_h(j_h u - u_h, w_h) \\ &= a(j_h u - u, w_h) + S_h(u, w_h) + S_h(j_h u - u, w_h), \end{aligned} \tag{3.12}$$

where we set $w_h := j_h u - u_h$ for abbreviation.

We start by estimating the first term on the right hand side of (3.12). Using the Cauchy–Schwarz inequality, the interpolation property (2.9) of j_h and the fact $c \in L^\infty(\Omega)$, it follows that

$$\begin{aligned} &\varepsilon\big(\nabla(j_h u - u), \nabla w_h\big) + \big(c(j_h u - u), w_h\big) \\ &\qquad\qquad \le C \left(\sum_{K\in\mathcal{T}_h} (\varepsilon + h_K^2) h_K^{2\lambda} \|u\|_{1+\lambda,K}^2 \right)^{1/2} |||w_h|||. \end{aligned} \tag{3.13}$$

In order to estimate the convective term in the bilinear form a, we integrate by parts and obtain

$$\begin{aligned} \big(\boldsymbol{b}\cdot\nabla(j_h u - u), w_h\big) = &- \big(j_h u - u, \boldsymbol{b}\cdot\nabla w_h\big) - \big(j_h u - u, w_h\,(\nabla\cdot\boldsymbol{b})\big) \\ &+ \big\langle(\boldsymbol{b}\cdot\boldsymbol{n})\,(j_h u - u), w_h\big\rangle_{\Gamma_N}. \end{aligned} \tag{3.14}$$

The three terms will be estimated separately. Using the orthogonality property (2.10) of the interpolation operator j_h, we get

$$\begin{aligned} \big(j_h u - u, \boldsymbol{b}\cdot\nabla w_h\big) &= \big(j_h u - u, \boldsymbol{b}\cdot\nabla w_h\big) - \big(j_h u - u, \pi_h(\boldsymbol{b}\cdot\nabla w_h)\big) \\ &= \big(j_h u - u, \kappa_h(\boldsymbol{b}\cdot\nabla w_h)\big). \end{aligned}$$

ETNA
Kent State University
etna@mcs.kent.edu

Using (3.10) and the approximation property (2.9), we estimate

$$\begin{aligned}
\left|\left(j_h u - u, \boldsymbol{b}\cdot\nabla w_h\right)\right| &\le \sum_{K\in\mathcal{T}_h} \|j_h u - u\|_{0,K}\,\|\kappa_h(\boldsymbol{b}\cdot\nabla w_h)\|_{0,K}\\
&\le C \sum_{K\in\mathcal{T}_h} h_K^{1+\lambda}\|u\|_{1+\lambda,K}\left(\|w_h\|_{0,K} + \|\kappa_h(\nabla w_h)\|_{0,K}\right)\\
&\le C\left(\sum_{K\in\mathcal{T}_h} h_K^{2+2\lambda}\,\|u\|^2_{1+\lambda,K}\right)^{1/2} \|w_h\|_0\\
&\quad + C\left(\sum_{K\in\mathcal{T}_h} h_K^{2+2\lambda}\,\tau_K^{-1}\|u\|^2_{1+\lambda,K}\right)^{1/2}\left(\sum_{K\in\mathcal{T}_h}\tau_K\|\kappa_h(\nabla w_h)\|^2_{0,K}\right)^{1/2}
\end{aligned}$$

and we obtain

$$\left|\left(j_h u - u, \boldsymbol{b}\cdot\nabla w_h\right)\right| \le C\left(\sum_{K\in\mathcal{T}_h} h_K^{1+2\lambda}\,\|u\|^2_{1+\lambda,K}\right)^{1/2} |||w_h|||, \tag{3.15}$$

where $c_0 > 0$ and the choice $\tau_K \sim h_K$ were exploited.

The second term in (3.14) can be estimated as follows

$$\left|\left(j_h u - u, w_h\,(\nabla\cdot\boldsymbol{b})\right)\right| \le C\left(\sum_{K\in\mathcal{T}_h} h_K^{2+2\lambda}\,\|u\|^2_{1+\lambda,K}\right)^{1/2} |||w_h|||, \tag{3.16}$$

where the interpolation error estimate (2.9), $\boldsymbol{b}\in\left(W^{1,\infty}(\Omega)\right)^d$, and $c_0 > 0$ were used.

Applying (3.9), the last term in (3.14) can be estimates as

$$\begin{aligned}
\left\langle(\boldsymbol{b}\cdot\boldsymbol{n})\,(j_h u - u), w_h\right\rangle_{\Gamma_N} &= \sum_{E\in\mathcal{E}_{h,N}} \left\|\,|\boldsymbol{b}\cdot\boldsymbol{n}|^{1/2}\,(j_h u - u)\right\|_{0,E}\left\|\,|\boldsymbol{b}\cdot\boldsymbol{n}|^{1/2}\,w_h\right\|_{0,E}\\
&\le C\left(\sum_{K\in\mathcal{T}_h} h_K^{2\lambda+1}\,\|u\|^2_{1+\lambda,K}\right)^{1/2} |||w_h|||,
\end{aligned} \tag{3.17}$$

where the shape regularity of $\mathcal{T}_h$ and $\boldsymbol{b}\in\left(W^{1,\infty}(\Omega)\right)^d$ were exploited. Putting together the estimates (3.15), (3.16), and (3.17), we get the bound

$$\left|\left(\boldsymbol{b}\cdot\nabla(j_h u - u), w_h\right)\right| \le C\left(\sum_{K\in\mathcal{T}_h} h_K^{2\lambda+1}\,\|u\|^2_{1+\lambda,K}\right)^{1/2} |||w_h||| \tag{3.18}$$

for the convective terms in the bilinear form a. Using (3.13) and (3.18), we conclude that

$$\left|a(j_h u - u, w_h)\right| \le C\left(\sum_{K\in\mathcal{T}_h} (\varepsilon + h_K)\,h_K^{2\lambda}\,\|u\|^2_{1+\lambda,K}\right)^{1/2} |||w_h||| \tag{3.19}$$

holds true.

The second term on the right hand side of (3.12) can be handled by Lemma 3.2. We get

$$\left|S_h(u, w_h)\right| \le C\left(\sum_{K\in\mathcal{T}} h_K^{2\lambda+1}\|u\|^2_{1+\lambda,K}\right)^{1/2} |||w_h|||. \tag{3.20}$$

ETNA
Kent State University
etna@mcs.kent.edu

To estimate the third term of (3.12), we use the Cauchy–Schwarz inequality, the L^2 stability of the fluctuation operator κ_h, the parameter choice $\tau_K \sim h_K$, and the approximation property (2.9) of the interpolation operator j_h. We obtain

$$
\begin{aligned}
S_h(j_h u - u, w_h) &\le S_h(j_h u - u, j_h u - u)^{1/2}\, S_h(w_h, w_h)^{1/2} \\
&\le \left\{ \sum_{K\in\mathcal{T}_h} \tau_K \|\kappa_h(\nabla(j_h u - u))\|_{0,K}^2 \right\}^{1/2} |||w_h||| \\
&\le C \left(\sum_{K\in\mathcal{T}_h} h_K^{2\lambda+1} \|u\|_{1+\lambda,K}^2 \right)^{1/2} |||w_h|||.
\end{aligned}
\tag{3.21}
$$

Using (3.12) and the estimates (3.19), (3.20), (3.21), we obtain

$$
|||j_h u - u_h||| \le C \left(\sum_{K\in\mathcal{T}_h} (\varepsilon + h_K)\, h_K^{2\lambda} \|u\|_{1+\lambda,K}^2 \right)^{1/2}.
$$

Combining this with (3.7) and (3.11) yields the assertion (3.5). The estimate for the case $u \in H^{s+1}(\Omega)$ follows the same lines. □

4. Numerical examples. This section will present some numerical results for the local projection stabilization applied to convection-diffusion problem. All numerical calculations were performed with the finite element package MooNMD [20].

We consider problems on the unit square $\Omega = (0,1)^2$. Our calculations were carried out on quadrilateral meshes which were obtained by successive regular refinement of an initial coarse grid (level 0) consisting of 4×4 congruent squares. The number of degrees of freedom

TABLE 4.1
Total number of degrees of freedom.

level	dofs		
	$Q_{1,h}^{\text{bubble}}$	$Q_{2,h}^{\text{bubble}}$	$Q_{3,h}^{\text{bubble}}$
0	41	113	201
1	145	417	753
2	545	1,601	2,913
3	2,113	6,273	11,457
4	8,321	24,833	45,441
5	33,025	98,817	180,993

for different enriched finite element spaces are given in Table 4.1. It is clearly to see that the number of dofs increases by a factor of about 4 from one mesh level to the next finer one.

Since $\tau_K \sim h_K$, compare Theorem 3.3, the stabilization parameters are chosen as follows

$$
\tau_K := \tau_0\, h_K \qquad \forall K \in \mathcal{T}_h,
$$

where $\tau_0 > 0$ denotes a constant which will be fixed for each of the test problems presented in this section.

We will investigate in this section the behaviour of the local projection stabilization applied to problems with different kinds of solutions. The presented examples, except the first one, can be found in [7, 26].

ETNA
Kent State University
etna@mcs.kent.edu

4.1. Smooth solution. We start with a problem which has a smooth solution and check the convergence orders which were predicted by Theorem 3.3. Let

$$\varepsilon = 10^{-7}, \quad \boldsymbol{b} = (2,3)^T, \quad c = 1,$$

and

$$\Gamma_N := \big\{(x,y) \in \partial\Omega \,:\, x = 1,\, 0 < y < 1\big\}, \qquad \Gamma_D := \partial\Omega \setminus \Gamma_N.$$

The right hand side f, the Dirichlet boundary condition g_D on Γ_D, and the Neumann boundary condition g_N on Γ_N are chosen, such that

$$u(x,y) = \sin(\pi x)\,\sin(\pi y)$$

is the solution of (2.1). Table 4.2 shows for the enriched quadrilateral elements of first,

TABLE 4.2
Errors $|||u - u_h|||$ and rates of convergence, $\tau_K = 0.1\, h_K$.

level	$(Q_{1,h}^{\text{bubble}}, P_{0,h}^{\text{disc}})$		$(Q_{2,h}^{\text{bubble}}, P_{1,h}^{\text{disc}})$		$(Q_{3,h}^{\text{bubble}}, P_{2,h}^{\text{disc}})$	
0	8.634e-2		1.515e-2		1.871e-3	
1	3.206e-2	1.429	2.241e-3	2.757	1.696e-4	3.464
2	1.166e-2	1.459	3.423e-4	2.711	1.506e-5	3.494
3	4.166e-3	1.485	5.632e-5	2.603	1.330e-6	3.501
4	1.477e-3	1.496	9.683e-6	2.540	1.174e-7	3.502
5	5.229e-4	1.499	1.694e-6	2.515	1.037e-8	3.501

second, and third order the error in the local projection norm $|||\cdot|||$ on different levels where $\tau_0 = 0.1$ was used. We see that the predicted convergence order of $r + 1/2$ is achieved in all cases. Moreover, we see that higher order finite elements give much more accurate results with less unknowns.

4.2. Solution with exponential layer. We will study now the behaviour of the local projection stabilization for a problem with an exponential boundary layer. Let

$$\varepsilon = 10^{-7}, \quad \boldsymbol{b} = (0,2)^T, \quad c = 0,$$

and

$$\Gamma_D := \partial\Omega, \qquad \Gamma_N := \emptyset.$$

The right hand side f and the Dirichlet boundary condition g_D are chosen, such that

$$u(x,y) = (2x-1)\,\frac{1 - \exp\left(\frac{2(1-y)}{\varepsilon}\right)}{1 - \exp\left(-\frac{2}{\varepsilon}\right)}$$

is the solution of (2.1). Note that the solution u exhibits an exponential boundary layer at $y = 1$. Figure 4.1 shows for the choice $\tau_0 = 0.1$ the numerical solution which was obtained by using the approximation space $Q_{1,h}^{\text{bubble}}$ and the projection space $P_{0,h}^{\text{disc}}$. Note that here and in all subsequent figures only the nodal values at the cell vertices are shown, i.e., the additional bubble part of the solution will not be shown. We see that the numerical solution shows no oscillations in the whole domain. Away from the exponential boundary layer, the numerical solution approximates the function $2x - 1$ which is the solution of the reduced problem.

ETNA
Kent State University
etna@mcs.kent.edu

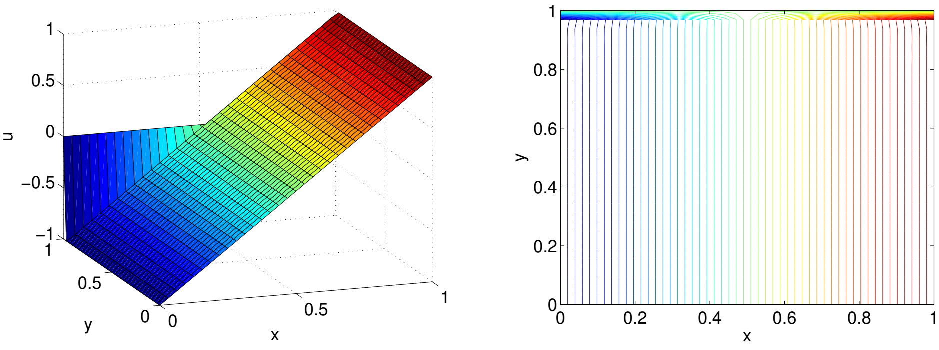

FIG. 4.1. *Example 4.2 with* $(V_h, D_h) = (Q_{1,h}^{bubble}, P_{0,h}^{disc})$ *and* $\tau_0 = 0.1$*: solution (left) and its isolines (right).*

4.3. Solution with interior and exponential layers. Our next problem is a benchmark for problems with an interior layer and an exponential layer. Let

$$\varepsilon = 10^{-7}, \quad \boldsymbol{b} = \big(8xy(1-x), -4(2x-1)(1-y^2)\big)^T, \qquad c = 0,$$

and

$$\Gamma_N := \big\{(x,y) \in \partial\Omega \,:\, 1/2 < x < 1,\, y = 0\big\}, \qquad \Gamma_D := \partial\Omega \setminus \Gamma_N.$$

We prescribe on Dirichlet boundary Γ_D the piecewise constant function

$$g_D(x,y) = \begin{cases} 1 & \text{for } 1/4 \le x \le 1/2\,,\ y = 0, \\ 1 & \text{for } 0 \le y \le 1\,,\ x = 1, \\ 0 & \text{otherwise,} \end{cases}$$

while the homogeneous Neumann condition $g_N = 0$ will be used on Γ_N. The right hand side in (2.1) is given by $f = 0$. The numerical solution for $\tau_0 = 0.01$ is presented in Figure 4.2.

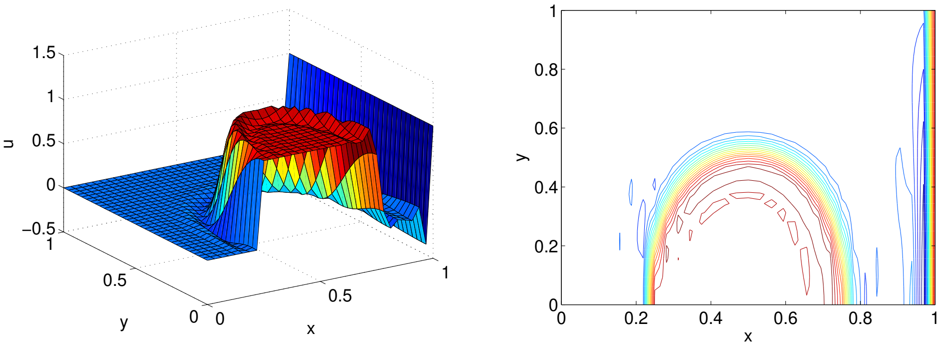

FIG. 4.2. *Example 4.3 with* $(V_h, D_h) = (Q_{1,h}^{bubble}, P_{0,h}^{disc})$ *and* $\tau_0 = 0.01$*: solution (left) and its isolines (right).*

It shows overshoots and undershoots near the interior layer and exponential boundary layer. This seems to be a common feature of many stabilization techniques; see [25]. However, the solution obtained by the local projection stabilization has no oscillations away from the

ETNA
Kent State University
etna@mcs.kent.edu

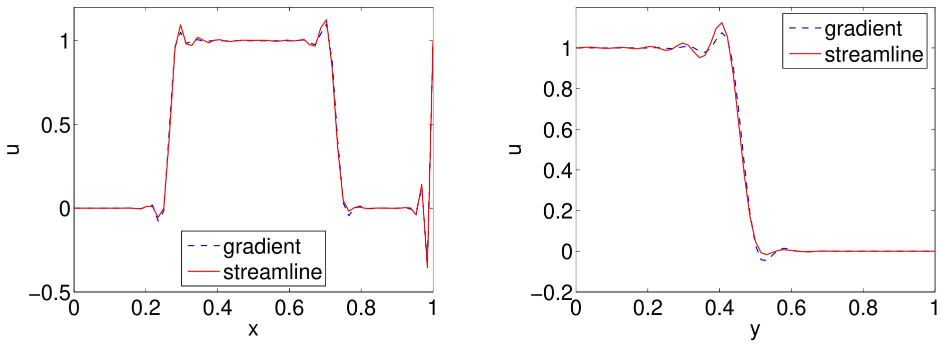

FIG. 4.3. *Example 4.3 with* $(V_h, D_h) = (Q_{1,h}^{bubble}, P_{0,h}^{disc})$ *and* $\tau_0 = 0.01$*: profiles along the lines* $y = 0.25$ *(left) and* $x = 0.375$ *(right) for two different stabilizations.*

layer. Furthermore, the position of the layers is captured very well. There are no significant differences between the numerical solutions obtained by using the stabilizing term (2.6) or its alternative based on the fluctuations of the derivatives in streamline direction; see Figure 4.3.

4.4. Solution with parabolic layers. The solution of our last example exhibits two parabolic boundary layers. Let

$$\varepsilon = 10^{-7}, \quad \boldsymbol{b} = (0, 1 + x^2)^T, \quad c = 0,$$

and

$$\Gamma_N := \big\{(x, y) \in \partial\Omega \,:\, 0 < x < 1,\, y = 1\big\}, \qquad \Gamma_D := \partial\Omega \setminus \Omega_N.$$

We use homogeneous Neumann condition $g_N = 0$ on Γ_N while the Dirichlet boundary condition g_D on Γ_D is given by

$$g_D = \begin{cases} 1 & \text{for } 0 \le x \le 1,\ y = 0, \\ 1 - y & \text{otherwise.} \end{cases}$$

Furthermore, the right hand side of (2.1) is $f = 0$. Note that the solution of (2.1) exhibits parabolic layers at the vertical walls $x = 0$ and $x = 1$. The pictures in Figure 4.4 show the obtained result for $\tau_0 = 0.01$. We see that the parabolic boundary layers are well captured. Overshoots and undershoots occur only near the layers while the solution has no oscillations away from the layer.

We are finally interested in the influence of the size of the stabilization parameter τ_K on the solution. To this end, we will vary the constant τ_0 in $\tau_K = \tau_0\, h_K$. For simplicial meshes and piecewise linears enriched with cubic bubbles, it is known that the elimination of the bubble part leads to the SUPG method where the stabilization parameters of both methods act in an inverse way; see [14]. For quadrilaterals, it is an open question and needs further theoretical studies. Exemplarily, we plot the solution on the outflow boundary. We start with calculation for the pair $(Q_{1,h}^{\text{bubble}}, P_{0,h}^{\text{disc}})$. The graphs in Figure 4.5 show that too small values for τ_0 result in oscillations while too large values for τ_0 cause a smearing of the layer. If the constant τ_0 is chosen suitably then the solution is captured very well on almost the whole edge. This means that the remaining small oscillations concentrate near the boundary and only a little smearing takes place.

ETNA
Kent State University
etna@mcs.kent.edu

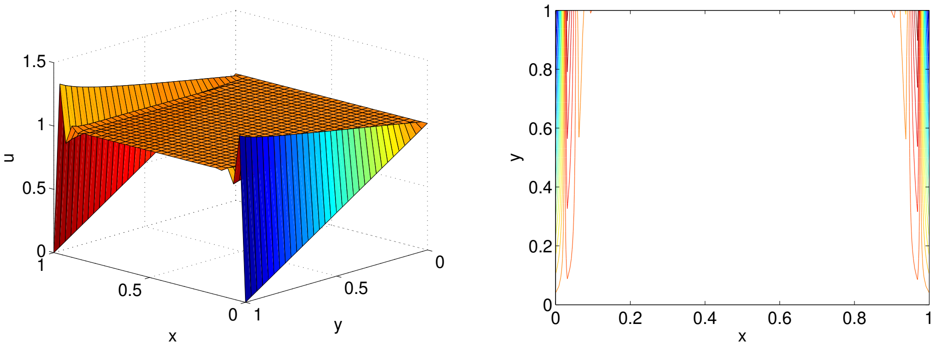

FIG. 4.4. *Example 4.4 with* $(V_h, D_h) = (Q_{1,h}^{bubble}, P_{0,h}^{disc})$ *and* $\tau_0 = 0.01$*: solution (left) and its isolines (right).*

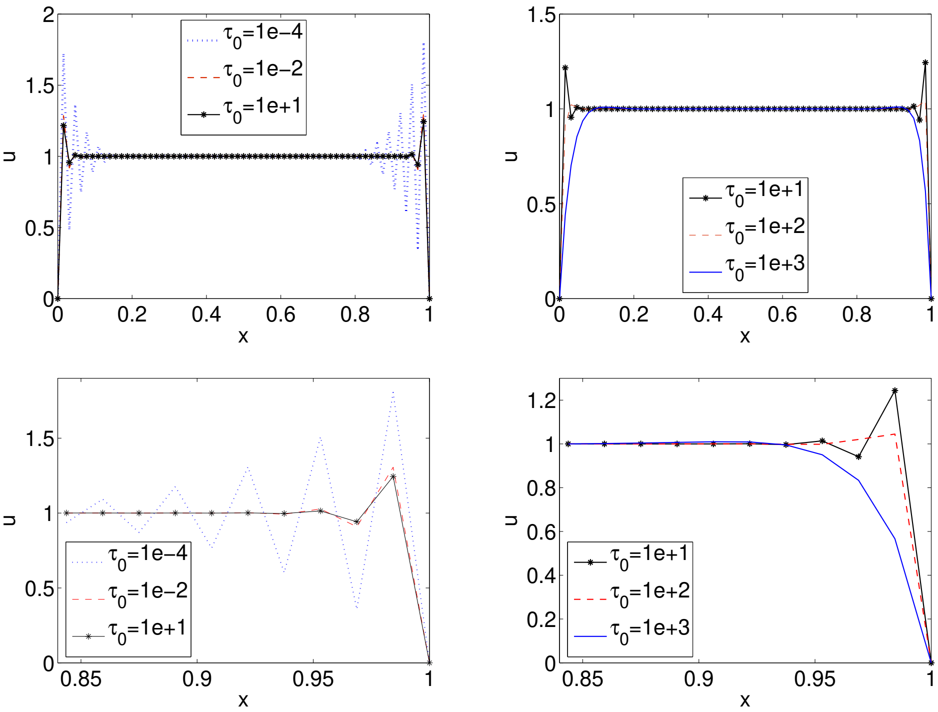

FIG. 4.5. *Example 4.4 with* $(V_h, D_h) = (Q_{1,h}^{bubble}, P_{0,h}^{disc})$*: Influence of parameter* τ_0 *on the behaviour of outflow profile.*

Using the pair $(Q_{2,h}^{\text{bubble}}, P_{1,h}^{\text{disc}})$, the situation changes. Even for the quite small stabilization parameter $\tau_0 = 0.01$, the solution shows no oscillations in the nodal values at the vertices; see Figure 4.6. One reason for this behaviour might be the additional stability which is already introduced by the presence of bubble functions in $Q_{2,h}^{\text{bubble}}$.

5. Conclusions. We have presented and analysed a stabilized finite element method for solving convection-diffusion problems. The stabilization was achieved by applying the local projection technique which gives additional control over the fluctuation of the gradient. Our analysis handles mixed boundary conditions. The given a-priori error estimate gives qualita-

ETNA
Kent State University
etna@mcs.kent.edu

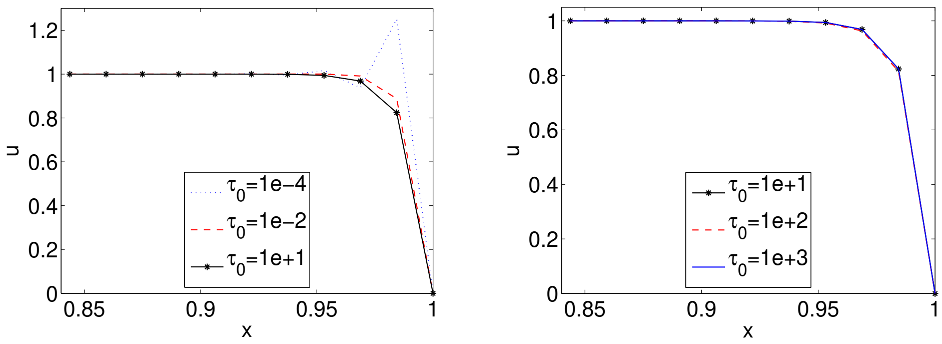

FIG. 4.6. *Example 4.4 with* $(V_h, D_h) = (Q_{2,h}^{bubble}, P_{1,h}^{disc})$*: Influence of parameter* τ_0 *on the behaviour of outflow profile.*

tively the same result as other stabilization techniques like the streamline diffusion method. The numerical results presented in Section 4 show that stabilization by local projection is well suited for problems with layers of different kind. The last example indicates that the size of the stabilization parameter has for first order elements an important influence on the quality of the numerical solution while the dependence is much smaller for second order elements.

REFERENCES

[1] L. E. ALAOUI, A. ERN, AND E. BURMAN, *A nonconforming finite element method with face penalty for advection-diffusion equations*, in Numerical Mathematics and Advanced Applications, Bermúdez de Castro, et al, eds., Springer, Berlin, 2006, pp. 512–519.
[2] D. N. ARNOLD, D. BOFFI, AND R. S. FALK, *Approximation by quadrilateral finite elements*, Math. Comp., 71 (2002), pp. 909–922.
[3] R. BECKER AND M. BRAACK, *A finite element pressure gradient stabilization for the Stokes equations based on local projections*, Calcolo, 38 (2001), pp. 173–199.
[4] ———, *A two-level stabilization scheme for the Navier-Stokes equations*, in Numerical Mathematics and Advanced Applications, M. Feistauer, et al, eds., Springer, Berlin, 2004, pp. 123–130.
[5] M. BRAACK AND E. BURMAN, *Local projection stabilization for the Oseen problem and its interpretation as a variational multiscale method*, SIAM J. Numer. Anal., 43 (2006), pp. 2544–2566.
[6] E. BURMAN, *A unified analysis for conforming and nonconforming stabilized finite element methods using interior penalty*, SIAM J. Numer. Anal., 43 (2005), pp. 2012–2033.
[7] H. C. ELMAN, D. J. SILVESTER, AND A. J. WATHEN, *Finite Elements and Fast Iterative Solvers: with Applications in Incompressible Fluid Dynamics*, Oxford University Press, New York, 2005.
[8] A. ERN AND J.-L. GUERMOND, *Theory and Practice of Finite Elements*, Applied Mathematical Sciences, vol. 159, Springer-Verlag, New York, 2004.
[9] M. FEISTAUER, *On the finite element approximation of functions with noninteger derivatives*, Numer. Funct. Anal. Optim., 10 (1989), pp. 91–110.
[10] L. P. FRANCA, *An overview of the residual-free-bubbles method*, in Numerical Methods in Mechanics (Concepción, 1995), C. Conca and G. N. Gatica, eds., Pitman Res. Notes Math. Ser., vol. 371, Longman, Harlow, 1997, pp. 83–92.
[11] L. P. FRANCA AND A. RUSSO, *Deriving upwinding, mass lumping and selective reduced integration by residual-free bubbles*, Appl. Math. Lett., 9 (1996), pp. 83–88.
[12] L. P. FRANCA AND L. TOBISKA, *Stability of the residual free bubble method for bilinear finite elements on rectangular grids*, IMA J. Numer. Anal., 22 (2002), pp. 73–87.
[13] S. GANESAN, G. MATTHIES, AND L. TOBISKA, *Local projection stabilization of equal order interpolation applied to the Stokes problem*, Math. Comp., 77 (2008), pp. 2039–2060.
[14] S. GANESAN AND L. TOBISKA, *Stabilization by local projection for convection-diffusion and incompressible flow problems*, J. Sci. Comput., published online December 18, 2008, DOI: 10.1007/s10915-008-9259-8.
[15] D. GILBARG AND N. S. TRUDINGER, *Elliptic Partial Differential Equations of Second Order*, Springer-Verlag, Berlin, 2001.

[16] P. GRISVARD, *Elliptic Problems in Nonsmooth Domains*, Monographs and Studies in Mathematics, vol. 24, Pitman (Advanced Publishing Program), Boston, MA, 1985.

[17] ———, *Singularities in boundary value problems*, Recherches en Mathématiques Appliquées (Research in Applied Mathematics), vol. 22, Masson, Paris, 1992.

[18] J.-L. GUERMOND, *Stabilization of Galerkin approximations of transport equations by subgrid modeling*, M2AN Math. Model. Numer. Anal., 33 (1999), pp. 1293–1316.

[19] T. J. R. HUGHES AND A. BROOKS, *A multidimensional upwind scheme with no crosswind diffusion*, in Finite Element Methods for Convection Dominated Flows (Collection of Papers Pres at Winter Annual Mtg of Asme, New York, Dec 2-7, 1979), T. J. R. Hughes, ed., American Society of Mechanical Engineers, New York, 1979, pp. 19–35.

[20] V. JOHN AND G. MATTHIES, *MooNMD—a program package based on mapped finite element methods*, Comput. Vis. Sci., 6 (2004), pp. 163–169.

[21] G. MATTHIES, *Mapped finite elements on hexahedra. Necessary and sufficient conditions for optimal interpolation errors*, Numer. Algorithm, 27 (2001), pp. 317–327.

[22] G. MATTHIES AND F. SCHIEWECK, *On the reference mapping for quadrilateral and hexahedral finite elements on multilevel adaptive grids*, Computing, 80 (2007), pp. 95–119.

[23] G. MATTHIES, P. SKRZYPACZ, AND L. TOBISKA, *A unified convergence analysis for local projection stabilisations applied to the Oseen problem*, M2AN Math. Model. Numer. Anal., 41 (2007), pp. 713–742.

[24] G. MATTHIES AND L. TOBISKA, *The inf-sup condition for the mapped Q_k-P_{k-1}^{disc} element in arbitrary space dimensions*, Computing, 69 (2002), pp. 119–139.

[25] H.-G. ROOS, M. STYNES, AND L. TOBISKA, *Numerical Methods for Singularly Perturbed Differential Equations. Convection–Diffusion and Flow Problems*, Springer Series in Computational Mathematics, vol. 24, Springer-Verlag, Berlin, 1996.

[26] Y.-T. SHIH AND H. C. ELMAN, *Iterative methods for stabilized discrete convection-diffusion problems*, IMA J. Numer. Anal., 20 (2000), pp. 333–358.